

# OPTIMIZATION OF PROCESS PARAMETERS FOR WOOD LASER ENGRAVING BASED ON TAGUCHI METHOD APPROACH

HUYEN NGUYEN-THI-NGOC<sup>1</sup>, THAI-VIET DANG<sup>2\*</sup>

<sup>1</sup>Department of Manufacturing Engineering, <sup>2</sup>Department of Mechatronics, School of Mechanical Engineering, Hanoi University of Science and Technology, Hanoi, Vietnam.

DOI: 10.17973/MMSJ.2023\_10\_2023053

\*viet.dangthai@hust.edu.vn

The paper presents the optimization of process parameters for wood laser engraving based on Taguchi method and analysis of variance (ANOVA). Laser diode mini machines using power source 10W is used for the experimental investigation process. The main parameters in the experimental wood surface laser engraving include such as: laser power (P), engraving speed (S), number of engraving lines per 1mm (L) and engraving head focal height (H). The surface geometrical dimensions while engraving, the engraving width (B) and the engraving depth (D) are main factors to determine the performance of engraving lines and the aesthetics of the product. The experiments were designed by the Taguchi L25 orthogonal array to analyze and obtain the important parameters. Then, to evaluate the optimal combination of parameters in the laser engraving process. The research results show that the influence of the factors P, S takes the leading role. Beside the two parameters L and H have a small influence on wood carving products. The optimization results prove that the combination of above factors at the correct values will give the most optimal set of parameters while maximizing the engraving depth (D) and minimizing the engraving width (B).

## KEYWORDS

Analysis of variance (ANOVA), laser engraving, Taguchi method, the optimization of process parameters.

## 1 INTRODUCTION

In recent years, laser technology's diverse uses in industry, metallurgy, medicine, and electronics have inspired widespread awe [Xie 2020]. In addition, this technique has a number of advantages over conventional procedures, including reduced sample contact, high precision, a low heat-affected zone, high speed, flexibility, adaptability, and self-control. In addition to simple automation and computer control, [Long 2020] has a short processing time and inexpensive cost. One of the most important reasons for the development of laser machining technology is their precise machining of complicated forms and diverse materials, including metal [Nguyen 2022], wood [Atwee 2023], polymer [Khan 2021], and leather [Gulbiniene 2021], etc...

Laser engraving is a procedure that belongs to the category of surface treatment [Kotadiya 2016]. It is a non-contact method in which a concentrated laser beam is absorbed by the material and turned into thermal energy on the surface, causing the material to vaporize and leave a mark [Saeheaw 2022]. Lasers meet a vast array of needs for engraving produced parts, for identifying procedures, for product information, for printing specific and distinctive logos, for engraving on jewelry and

gems, for barcode printing, and for enhancing security [Long 2020]. In addition, unlike wood carving or painting techniques, laser engraving does not require oil and ink and may be used on a wide range of materials, such as metals, plastics, ceramics, glass, wood, and leather, as well as painted and emulsified surfaces [Kotadiya 2016].

Many lasers, such as CO2 lasers, diode lasers, UV lasers, and Fiber lasers, are utilized in the engraving industry [Long 2020]. One of the most practically important responsibilities is choosing the ideal parameter set to optimize the performance of the laser cutting process. The effect of laser control elements on the material must be regarded as a crucial factor in order to boost product quality and output. The research conducted by Pradhan et. al investigated the effects of the power factor on the surface roughness of metallic materials [Pradhan 2009]. Yet, high cutting speeds would raise up the the cutting temperature. The life expectancy of the cutting tool would diminish. Hence, the dimensional accuracy and surface roughness were compromised. In their paper, Kotadiya et al. explained about process parameters such as cutting speed, laser power, gas pressure, pulse frequency, beam diameter, and focus positions all contribute to the overall quality of laser cutting [Kotadiya 2016]. Gvozdev et al. provided a trustworthy approach for predicting cutting surface quality and selecting the best possible beginning parameters. Unfortunately, the optimization process for a high-quality cutting surface has taken a long period [Gvozdev 2015].

There are a number of successful uses of DOE (Design of Experiment) methods, including the Taguchi method and the Response Surface Method (RSM) [Rohith 2022]. The number of experiments could be cut in half with the Taguchi approach, as opposed to RSM's [Korgal 2022]. In addition, the Taguchi technique allows for the simultaneous analysis of several process parameters and the impact of those parameters [Long 2020]. Much of the work involved in laser-assisted milling is dedicated to locating the heat-affected zone so that the machined surface can be brought back to its original state. However, contour and product deformation are more likely to occur with soft materials that have high adhesion, such as wood, plastic, leather, etc.

Thus, this study provides the best combination of technological factors for the wood's surface by using Taguchi array design and analysis of variance. The depth and width of an engraving in woodcarving determine the product's light and dark tones. As laser power rises, engraving breadth and machining depth rise as well. When carving an image into wood, for example, a shallow depth will cause the picture to appear blurry and out of focus if the surface area is increased. The study's findings demonstrate that the influence parameters can be optimized to guarantee high-quality woodcarvings with desirable engraving width and depth, as well as the capacity to adapt to intricate designs.

## 2 METHODOLOGY

Because the study describes the optimization of process parameters for wood laser engraving using the Taguchi method and analysis of variance (ANOVA). The authors begin by discussing the significance of the Taguchi method in wood laser diode engraving. The Taguchi method is then combined with ANOVA to determine the optimal process parameters.

### 2.1 Taguchi Method

The Taguchi technique [Nguyen 2022], which is based on the design of experiments, is an efficient method for optimizing process parameters. Conventional experimental design concentrates primarily on the average value of the quality

characteristic. But orthogonal arrays (OA) can reduce the variation of the quality characteristic under investigation. Rather of relying on an average value, the Taguchi method uses the signal-to-noise (S/N) ratio to quantify the multiple experiments' results. The robustness measured by this ratio between the mean (signal) and the standard deviation (noise) is applied to the task of identifying the determinants of process variability and so mitigating the impact of external influences. During studies, measured responses are translated into appropriate S/N ratios using three generic classes, namely "larger-is-better, in Equation 1" "smaller-is-better, in Equation 2" and "nominal-is-best, in Equation 3", respectively. Use the following equations to calculate the S/N ratios for various sorts of quality attributes such as follows:

$$S/N(\eta_i) = -10 \log_{10} \left( \frac{1}{n} \sum_{i=1}^n \frac{1}{x_{ij}^2} \right) \quad (1)$$

$$S/N(\eta_i) = -10 \log_{10} \left( \frac{1}{n} \sum_{i=1}^n x_{ij}^2 \right) \quad (2)$$

and  $S/N(\eta_i) = -10 \log_{10} \left( \frac{\mu^2}{s^2} \right) \quad (3)$

where n is the number of trials;  $x_{ij}$  is the measured response value for the j<sup>th</sup> quality characteristic with respect to the i<sup>th</sup> trial; s is the mean and standard deviation of the responses for the given factor-level combination.

## 2.2 Experimental System

The experiment was conducted on a 4-axis mini laser engraving machine, with a maximum power of 10W, using a wavelength of 450nm, the engraving machine was controlled on a computer by GRBL Laser software, and engraved on the engraved sample with a framework of 50x50mm, in Figure 1.

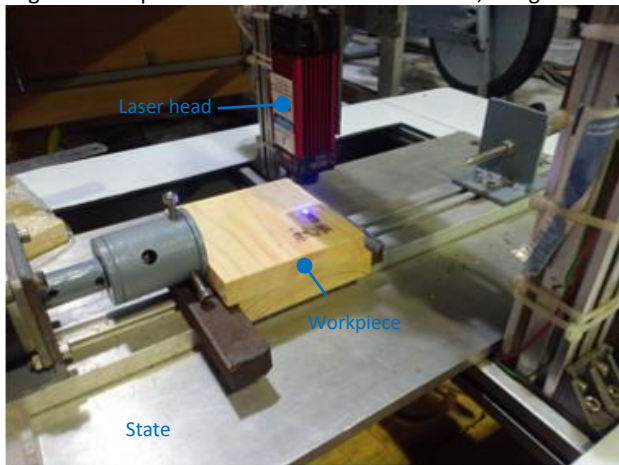


Figure 1. Engraving wood laser 4 axis mini machine.

The workpiece is pine wood with chemical composition shown in the Table 1.

C	O	H	N	Others (Ca,Ka,Na,Mg,...)
50%	42%	6%	1%	1%

Table 2. Chemical composition of pine wood.

Using the L25 orthogonal array, the Taguchi design of the test technique was implemented to determine the effect of each input parameter on the output attributes. Engraving speed, number of lines per 1mm, focal length, and energy are the primary parameters affecting the machining process. Experiments were conducted in advance to establish a parameter range. These are the ranges for speed and power scanning:

- Power: 1.5 W to 5.5W.

- Machine speed: 100mm/min to 2000 mm/min.
- Number of lines can be adjusted from 6 to 10 engraving lines / 1 mm.
- The focal length of the engraving head is adjustable from 20 to 45 mm.

Table 2 displays the factor levels and processing conditions.

Parameter	Value Level				
	1	2	3	4	5
Energy (P) (W)	1,5	2,5	3,5	4,5	5,5
Speed (S) (mm/min)	1200	1400	1600	1800	2000
Engraving lines (L) /mm	6	7	8	9	10
Focal length (H)	20	25	30	35	40

Table 2. The factor levels and processing conditions.

## 3 RESULTS AND DISCUSSION

In this study, engraving speed, focal length, number of n engraving lines per 1mm and effective power at five different levels were selected as control factors.



Figure 3. Engraved wood samples.

Using the Taguchi L25 orthogonal test layout, a total of 25 experiments were performed to determine the etching width (B) and engraving depth (D) values. With the above parameters, we proceed to engrave on wood samples as shown in Figure 3.



Figure 4. A KRUSS microscope 4X magnification.

Then conduct inspection and measure the dimensions of depth (D), engraving width (B) through a KRUSS microscope in Figure 4 with 4X magnification. After connecting the jack to the KRUSS microscope, samples are placed beneath the microscope and observed through the computer screen in order to conduct

measurements. As shown in Figure 5, we use a normal ruler on the computer screen to measure the appropriate dimensions D and B. With crater-like undulations, we will accept great depths.

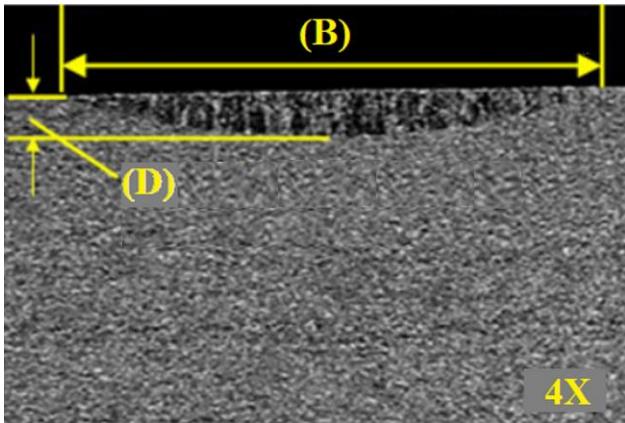


Figure 5. The dimensions D and B in the measurement process.

Figure 6 depicts a few actual images when measured and presented on the computer screen.

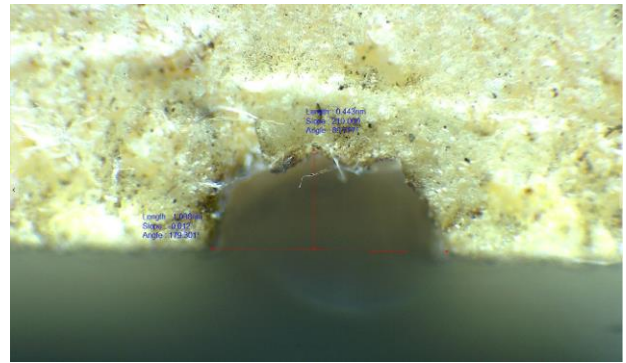
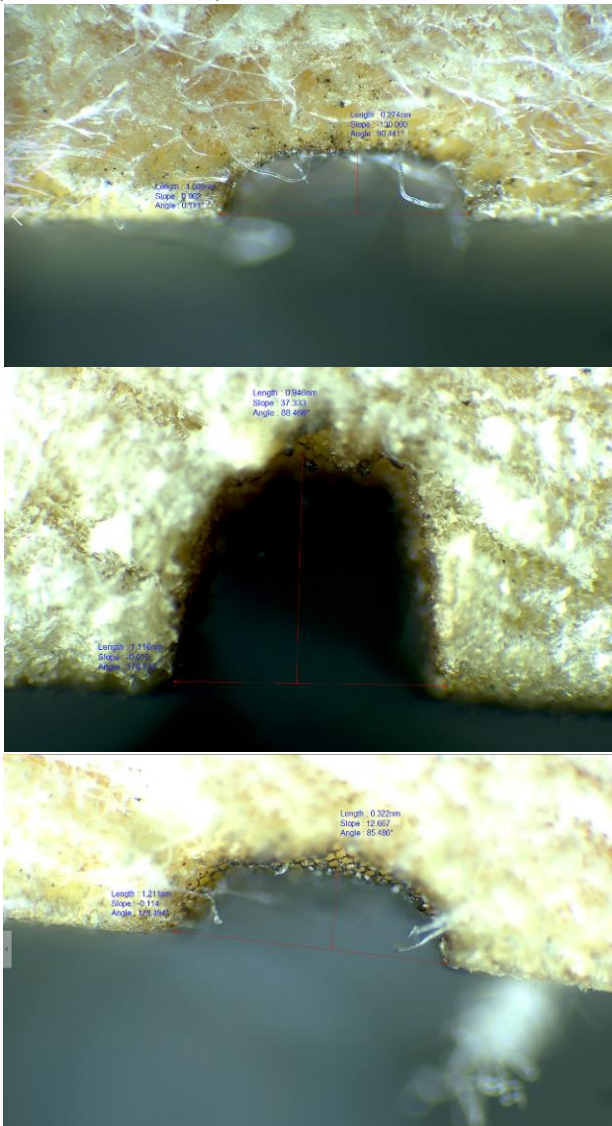


Figure 6. Determining the surface depth, width and angle of the test samples.

The results after measurement are summarized in Table 3.

No	Process parameter level				Responses	
	P (W)	S (mm/min)	L(line/mm)	H (mm)	D (mm)	B (mm)
1	1	1	1	1	0.163	1.089
2	1	2	2	2	0.153	0.985
3	1	3	3	3	0.131	1.035
4	1	4	4	4	0.084	0.990
5	1	5	5	5	0.021	0.998
6	2	1	2	3	0.443	1.038
7	2	2	3	4	0.388	1.061
8	2	3	4	5	0.322	1.211
9	2	4	5	1	0.477	1.087
10	2	5	1	2	0.170	0.995
11	3	1	3	5	1.435	1.108
12	3	2	4	1	0.946	1.116
13	3	3	5	2	0.497	1.038
14	3	4	1	3	0.633	1.030
15	3	5	2	4	0.274	1.089
16	4	1	4	2	1.246	1.079
17	4	2	5	3	1.296	1.090
18	4	3	1	4	0.747	1.180
19	4	4	2	5	0.304	1.134
20	4	5	3	1	0.591	1.040
21	5	1	5	4	1.591	1.205
22	5	2	1	5	1.079	1.024
23	5	3	2	1	1.416	1.044
24	5	4	3	2	0.953	1.075
25	5	5	4	3	1.053	1.068

Table 3. The response value after completed measurement.

### 3.1 Effect of processing conditions on engraving depth D

Figure 7 depicts the examination of the influence of the parameter set on the engraving depth D from the obtained data in Table 3.

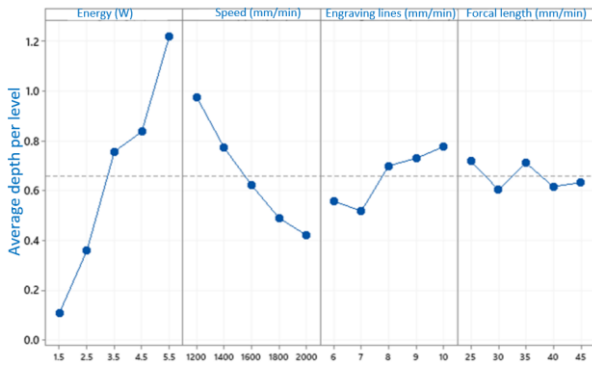


Figure 7. The influence of the processing conditions on the engraving depth D.

The results show that the each factor's influence on the engraving depth, the cutting energy that has the greatest influence on the engraving depth also increases, the number of engraving lines and the focal length have a small influence when increasing or decreasing. Figure 8 shows that when the two factors, the number of lines at 8 (Line/mm) and the focal length (35mm) are fixed, and when the power level is increased, the engraving depth also increases and the engraving speed increases. then the engraving depth is reduced, in addition, Figure 8 also shows the highest depth for high energy and low speed, the smallest depth for low energy and high speed.

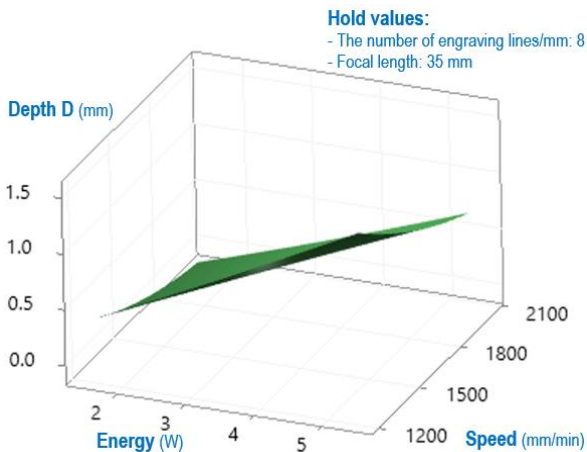


Figure 8. The Chart of the processing conditions effecting on the engraving depth D.

Figure 9 is the change of energy and number of engraving lines/mm in an increasing direction, while the two speed and focal factors are assigned values at 1600mm/min and 35mm respectively, Figure 9 shows the value. depth value increases with increasing energy value and number of engraving lines, Figure 9 also shows the lowest depth at the lowest energy and the fewest number of lines/mm, the highest depth when the energy level is highest and the maximum number of engraving lines/mm.

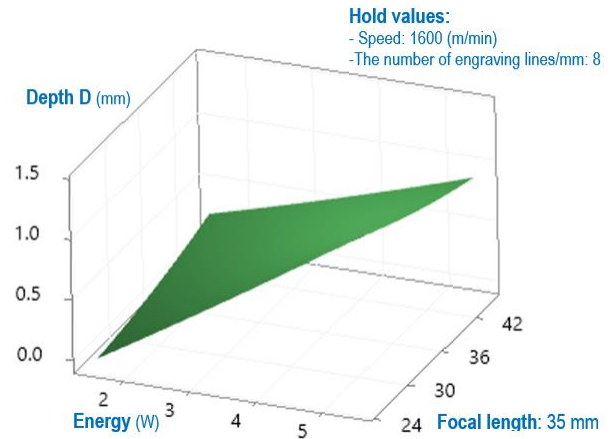


Figure 9. The Chart of the processing conditions effecting on the engraving depth D, while increasing Energy and Speed.

Figure 10 has a changed profile quite similar to Figure 9. In this Figure 10 chart, two factors of Speed and Number of engraving lines/mm are kept at 1600 mm/min and 8 Line/mm. Energy level and Focal length are changed such as follows: when energy increases in order to raise up depth D. Increasing focal length at low power will increase depth D. But, high Energy makes depth D will be decreased. The lowest value of depth is at low Energy and low Focal length, the highest depth value is at the highest energy and lowest focal length.

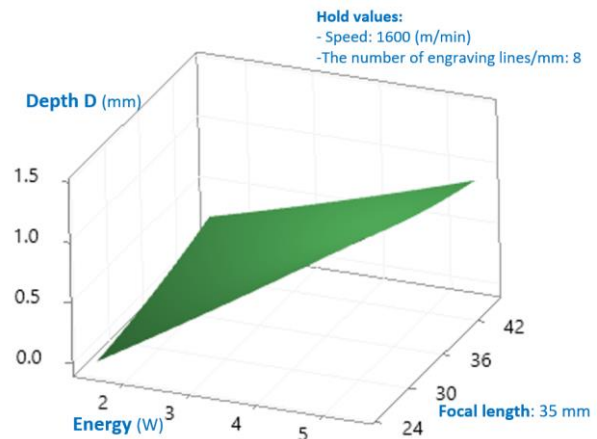
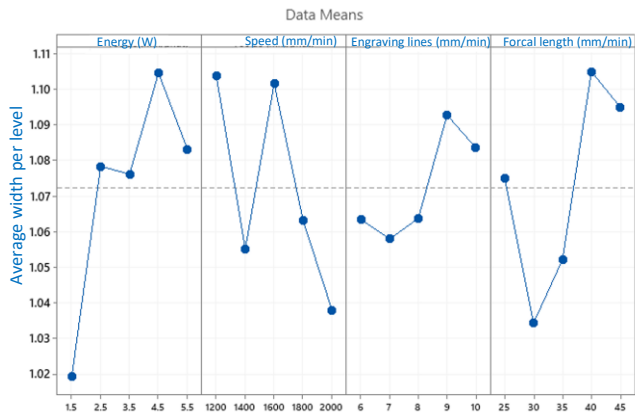


Figure 10. The Chart of the processing conditions effecting on the engraving depth D, while changing P and H, remaining S and L.

After completing the investigation of the influence of the processing conditions on the engraving depth D. The authors continue to investigate the influence on the engraving width B, in the Subsection 3.2.

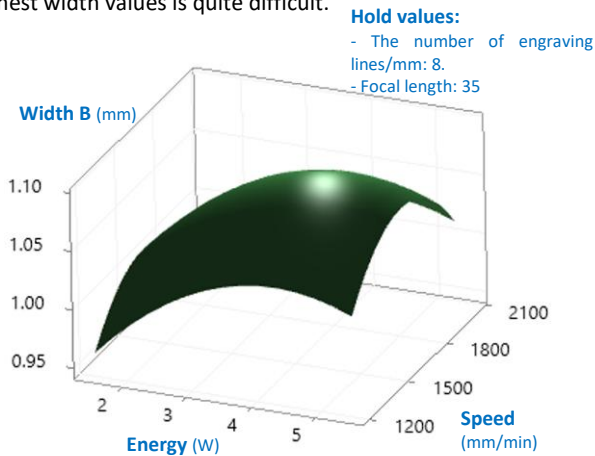
### 3.2 Effect of processing conditions on engraving width B

Figure 11 shows that the energy and speed do not change the width value in an increasing or decreasing direction, but it changes the width price up and down unevenly like the other two factors. The width value changes strongly and abnormally when increasing the power level from 1.5W-2.5W, speed from 1200-1600 mm/min, number of engraving lines/mm from 8-9 Line/mm, focal length from 35-40 mm. Because of the difference between the 2D charts, the 3D histograms in terms of width also have a different change compared to the 3D charts in Figures 8-10, if Figures 8-10 is 3D histograms in the form of If the plane is warped, Figures 14-16 is a clear curved surface 3D histogram.



**Figure 11.** The influence of the processing conditions on the engraving width B.

Similar to the depth of 3D charts in terms of width, Figure 12-14 is also arranged as shown in Figures 8-10, and especially in all these three charts, although they have different profiles, the factors when changing All values make the width change unevenly and continuously, so determining the lowest and highest width values is quite difficult.



**Figure 12.** The influence of the processing conditions on the engraving width B while changing P and S, remaining L and H.

Only in the 3D chart in Figure 13, the number of engraved lines increases, causing the width to increase.

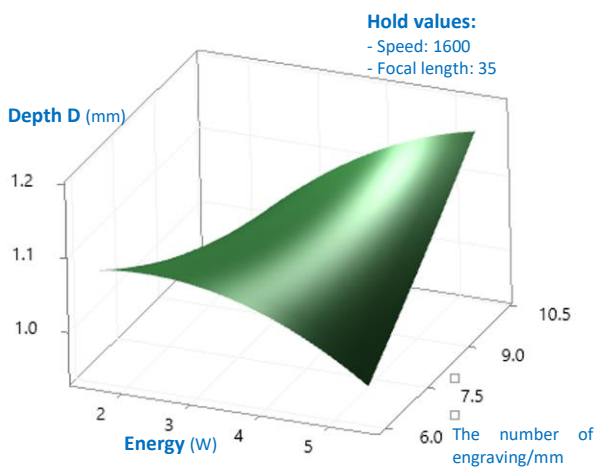


**Figure 13.** The influence of the processing conditions on the engraving width B while changing P and L, remaining S and H.

Accordingly, the lowest width is determined at the highest energy level and the lowest number of markings, the highest width corresponds to the highest energy level and the maximum number of markings.

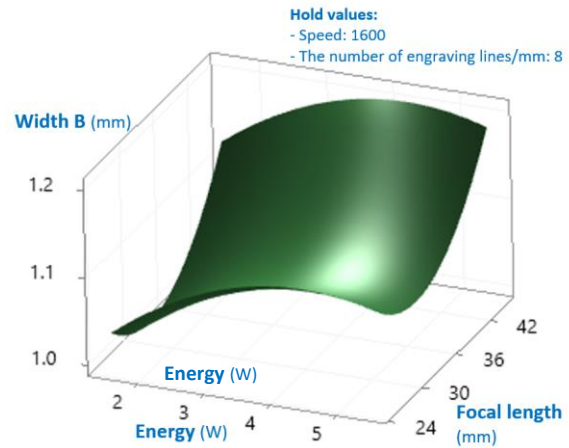


**Figure 14.** The influence of the processing conditions on the engraving width B while changing P and H, remaining S and L.

### 3.3 Optimization of processing parameters

Based on the aid of Equations 1 to 3, The multi-response S/N ratio is given by as follows:

$$\eta = \omega_1 \eta_1 + \omega_2 \eta_2 \quad (4)$$

where  $\omega_1$  and  $\omega_2$  are the weighting factors related to the S/N ratio for each D and B response, respectively. These weighting factors are decided on the basis of priorities between different reactions that are optimized simultaneously. In this experiment, 0.5 weighting factors for each response are considered, which give equal priority to both D and B for concurrent optimization. The calculated values of the S/N ratio for each response and the multi-response S/N ratio for each test in the orthogonal array are given in Table 4.

No	Process parameter level				S/N ratio		
	P (W)	S (mm/min)	L (line/mm)	H (mm)	S/N <sub>D</sub>	S/N <sub>w</sub>	S/average(N)
1	1	1	1	1	15.783	0.737	8.260
2	1	2	2	2	16.306	-0.131	8.087
3	1	3	3	3	17.655	0.299	8.977
4	1	4	4	4	21.514	-0.087	10.714
5	1	5	5	5	33.556	-0.017	16.769
6	2	1	2	3	7.072	0.324	3.698
7	2	2	3	4	8.223	0.514	4.369
8	2	3	4	5	9.843	1.663	5.753
9	2	4	5	1	6.430	0.725	3.577
10	2	5	1	2	15.391	-0.044	7.674
11	3	1	3	5	-3.137	0.891	-1.123
12	3	2	4	1	0.482	0.953	0.718
13	3	3	5	2	6.073	0.324	3.198
14	3	4	1	3	3.972	0.257	2.114
15	3	5	2	4	11.245	0.741	5.993
16	4	1	4	2	-1.910	0.660	-0.625
17	4	2	5	3	-2.252	0.749	-0.752
18	4	3	1	4	2.534	1.438	1.986
19	4	4	2	5	10.343	1.092	5.717
20	4	5	3	1	4.568	0.341	2.454
21	5	1	5	4	-4.033	1.620	-1.207
22	5	2	1	5	-0.660	0.206	-0.227

23	5	3	2	1	-3.021	0.374	-1.324
24	5	4	3	2	0.418	0.628	0.523
25	5	5	4	3	-0.449	0.571	0.061

**Table 4.** The multi-response S/N ratio based on the process parameter level.

Using the signal-to-noise ratio afforded by the Taguchi technique, we were able to obtain a set of parameters comprising all 25 experiments and thereby calculate the percentage influence of four factors: energy level; speed; number of lines engraved; and focal length; and five levels of adjusted values by the following equation 5 as follows:

$$5(m_{j1} - m)^2 + 5(m_{j2} - m)^2 + 5(m_{j3} - m)^2 + 5(m_{j4} - m)^2 + 5(m_{j5} - m)^2 \quad (5)$$

where  $m_{ji}$  : The average of the average S/N ratio in the same factor including 5 different values;  $m$  : The average of the average S/N ratio in 25 different values.

From Equation (5) yields the ANOVA's table 5.

Factor	The ratio S/N per each level					Sum of squares	Influence %
	1	2	3	4	5		
P	10.561	5.014	2.180	1.756	-0.435	359.609	78%
S	6.590	2.439	3.718	4.529	1.801	70.865	15%
L	3.961	4.434	3.040	3.324	4.317	7.494	2%
H	2.737	3.772	2.820	4.371	5.378	24.528	5%

**Table 5.** ANOVA table

Based on the results of the ANOVA table, it is obvious that the energy level has a substantial effect on engraving quality (by a percentage of 78%), followed closely by the engraving speed. 15%, with the remaining 5% and 2% coming from the number of lines and the focus length, respectively. Nevertheless, in reality, the energy level and the focal length do not effect the engraving time; rather, the engraving time varies directly with the speed at which the engraving is performed and with the number of lines engraved. That allows us to tailor the settings to each individual client's preferences. The ANOVA spreadsheet not only shows us how much each parameter changes the engraving process, but it also suggests which parameters to tweak to get the best results.

The best parameters were chosen by calculating the average of S/N ratios for each of the five levels of values (called  $m_{ji}$ ) in the ratio factors over all rows. which, as noted in red colour on the ANOVA spreadsheet (see Table 5), is the ideal set of parameters to be chosen:

Factor	Optimized S/N	Level	The corresponding value level
P	-0.435	5	450 W
S	1.801	5	2000 mm/min
L	3.040	3	8 line/mm
H	2.737	1	25 mm

**Table 6.** The set of optimized process parameters.

The validation will be performed by comparing the optimal set of parameters to the sets of parameters at the minimum, maximum, and adjacent optimal levels shown in Table 7. The Figure 15 of Lotus flower illustrates the feasibility of the set of optimized process parameters to the performance of wood laser engraving products. The result of optimized process

parameters in Table 6 combines with the comparison results in Table 7 prove the performance of Figure 15a is the best.

Factor	Optimized	Minimum	Maximum	Neighbor 1	Neighbor 2	Neighbor 3
P	550	150	550	450	350	250
S	2000	2000	1200	1800	1200	1400
L	8	6	10	7	6	9
H	25	25	25	30	40	35

**Table 7.** The comparison with the optimized process parameters

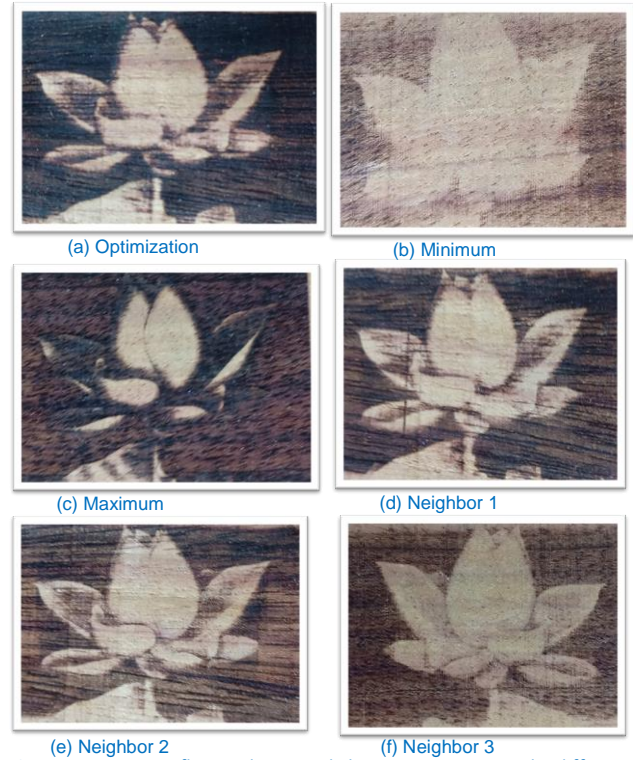


**Figure 15.** Lotus flower by wood laser engraving with different processing parameters.

Figure 15b - Minimum: The image is engraved with low power mode and high engraving speed, so it is not clear, almost only the outline of the flower. From the influence percentage spreadsheet, we can also see the power and speed has the greatest influence on the quality of the output results; the lower the power and the higher the speed, the poorer the engraving quality. Figure 15c - Maximum: Like the minimum parameter set, the maximum parameter set combines the parameter set with the highest power and the smallest engraving speed, practically burning the picture quality during the engraving process. Figure 15c shows the actual image we get when we engrave at the maximum settings; the engraving looks like black fire streaks. Figures 15 d, e, and f show neighbor 1, 2, and 3 parameter sets, which are not the best parameter set but are close enough that the etched picture will still look excellent. The output quality of this neighborhood set is extremely close to that of the optimal set of parameters, therefore the real image quality is highest in Neighborhood 1, then Neighborhood 2, and finally Neighborhood 3. This is especially evident when we compare our ANOVA spreadsheet's rank table with the rank table of the parameter sets. Figure 15a – Optimization: Through the process of experiment and calculation, the set of optimal parameters that we obtain will ensure the best output result, which is the combination of input values of power., speed, focal length and number of engravings per 1mm make the depth and width values always the best. On the basis of taguchi method and ANOVA analysis,

we can not only find out the percentage influence of each input parameter but also find the most optimal set of parameters. Actual images when engraving with the optimal set of parameters show that the engraving image quality is the best compared to the remaining sets, consistent with the research results and the reliability of the selected method.

#### 4 CONCLUSIONS

The use of Taguchi and Anova techniques has helped us determine the relative strengths of the various engraving process parameters; for example, we know that the energy level can affect the process by as much as 78%. As the engraving process is only little affected by the other two focal length parameters and the number of engraving lines/mm, these two values can be left at their ideal level even when using the engraving machine on different materials. The next engraving speed is 12%. More research will be conducted to see if a bigger capacity engraving head is necessary for materials other than wood, such as stainless steel, aluminum, etc. in order to obtain the best possible values, it should be treated like wood. The obtained results will contribute to the development of Vietnamese sculpting and shaping on wood.

#### REFERENCES

- [Xie 2020] Xie, L. et. Al. 2020 "Experimental Research on the Technical Parameters of Laser Engraving." *Journal of Physics Conference Series* 1646(1):012091.
- [Long 2020] Long, J.Q., Huang, W., Xiang, J. and Zhou, J. 2020 "Parameter Optimization Using Multi-objective Taguchi Method and Response Surface Methodology for the Laser Welding of Dissimilar Materials." *Lasers in Engineering* 39(3-6):225-241.
- [Nguyen 2022] Nguyen, V., Altarazi, F., and Tran, T. 2022. "Optimization of Process Parameters for Laser Cutting Process of Stainless Steel 304 A Comparative Analysis and Estimation with Taguchi Method and Response Surface Methodology." *Mathematical Problems in Engineering* 2022: Article ID 6677586.
- [Atwee 2023] Atwee, T., Swidan, A., Zahra, N. 2023. "An Overview Study on Laser Technology and Conventional Technology's Effect on Wood and Sheet Metal Manufacturing for The Furniture Industry Introduction." *International Design Journal* 13(2): 287-299.
- [Khan 2021] Khan, M. M. A, Saha, S., Romoli, L. and Kibria, M. H. 2021. "Optimization of Laser Engraving of Acrylic Plastics from the Perspective of Energy Consumption, CO<sub>2</sub> Emission and Removal Rate." *Journal of Manufacturing and Materials Processing* 5(3), 78.
- [Gulbiniene 2021] Gulbiniene, A. et. al. 2021 "Effect of CO<sub>2</sub> laser treatment on the leather surface morphology and wettability." *Journal of Industrial Textiles* 51(2): 2483S-2498S.
- [Kotadiya 2016] Kotadiya, D. J., and Pandya, D. H. 2016. "Parametric analysis of laser machining with response surface method on SS-304," *Procedia Technology* 23: 376-382.
- [Saeheaw 2022] Saeheaw, T. "Application of integrated CRITIC and GRA-based Taguchi method for multiple quality characteristics optimization in laser-welded blanks." *Heliyon* 8(2022): e11349.
- [Pradhan 2009] Pradhan, M. K., and Biswas, C. K. 2009. "Influence of process parameters on surface roughness in EDM of AISI D2 Steel: an RSM approach," *International Conference Emerging Research in Advanced Mechanical Engineering* 1(9): 709-714.
- [Gvozdev 2015] Gvozdev, A. E., and Golyshev, A. G. 2015. "Multiparametric optimization of laser cutting of steel sheets," *Inorganic Materials: Applied Research* 6(4): 305-310.
- [Rohith 2022] Rohith, S., Mohan, N., Malik, V., Kuldeep, K. S., Prasad, M. A. 2022. "Modelling and optimization of selective laser melting parameters using Taguchi and super ranking concept approaches." *International Journal on Interactive Design and Manufacturing* 2022: 1-13.
- [Korgal 2022] Korgal, G., Upadhyaya, S., Anilkumar, T. 2022. "Grain refinement of aluminium 4032 alloy with the impact of vibration using Taguchi technique and analysis of variance (ANOVA)." *Materials Today: Proceedings* 54 (2022): 507–512. proceedings including place and date of conference, Place: Publisher, page numbers (first-last), ISBN (if applicable).

#### CONTACTS:

Huyen Nguyen-Thi-Ngoc and Thai-Viet Dang  
School of Mechanical Engineering, Hanoi University of Science and Technology  
10000, Hanoi, Viet nam.  
huyen.nguyenthingoc@hust.edu.vn and viet.dangthai@hust.edu.vn